Stress-induced martensitic transformation in high-strength [236]-oriented $Ni_{51}Ti_{36.5}Hf_{12.5}$ single crystals

2015 IOP Conf. Ser.: Mater. Sci. Eng. 93 012047

(http://iopscience.iop.org/1757-899X/93/1/012047)

Stress-induced martensitic transformation in high-strength [236]-oriented $Ni_{51}Ti_{36.5}Hf_{12.5}$ single crystals

N Y Surikov, A S Eftifeeva, E Yu Panchenko and Yu I Chumlyakov

Tomsk State University, Siberian Physical-Technical Institute, Tomsk, 634050, Russia

E-mail: Jet_n@mail.ru, anna_eftifeeva@rambler.ru, panchenko@mail.tsu.ru, chum@phys.tsu.ru

Abstract. The effects of heat treatment on the stress-induced B2-B19' martensitic transformations in the $Ni_{51.0}Ti_{36.5}Hf_{12.5}$ single crystals oriented along [236] direction are studied. It is shown that in the annealed at 1323K for 4 h crystals, the temperature range of superelasticity increase almost twofold from 75K up to 135K as compared to the as-grown single crystal contained disperse particles of H-phase. The [236]-oriented $Ni_{51.0}Ti_{36.5}Hf_{12.5}$ single crystals are characterized with high levels of applied compressive stress up to 1700 MPa in the as-grown state and 1900 MPa in annealed crystals for the completely reversible stress-induced B2-B19′ martensitic transformation with reversible strain up to $|\varepsilon_{SE}|$ =1.4%.

1. Introduction

Alloys of TiNiHf undergoing reversible B2-B19′ martensitic transformation at high temperatures of above 100°C and high level of applied stress of above 1000 MPa [1-4] can find the wide range of practical applications in modern technologies. It is known that precipitation of disperse particles in the Ni-rich TiNi and NiTiHf alloys allows controlling characteristic transformation temperatures, the strength of the B2-phase due to precipitation hardening processes and increase cycle stability of such functional properties as the shape memory effect and superelasticity [1-5]. Up to the present there are no systematic studies of effects of dispersed particles on shape memory effect and superelasticity in high-strength TiNiHf alloys with Ni content greater than 50.5 at.%.

Therefore, the main objective of this work is to investigate dependence of the critical stress level for stress-induced martensitic transformation, temperature range of superelasticity response on microstructure of single crystals of the $Ni_{51.0}Ti_{36.5}Hf_{12.5}$ (at.%) alloy. Carrying out researches on NiTiHf single crystals allows, first, excluding the effect of grain boundaries on the allocation of the dispersed particles and on the development of the martensitic transformation. The second, it allows choosing the crystal orientation along [236] direction, which is characterized by maximum theoretical lattice strain $|\varepsilon_{tr0}|_{[236]}$ = 8.0% at B2-B19′ martensitic transformation in compression [3].

2. Experimental procedure

Single crystals of $Ni_{51.0}Ti_{36.5}Hf_{12.5}$ (at. %) alloy were grown by the Bridgman technique in an inert gas atmosphere. Electro-discharge machining was utilized to cut rectangular compression specimens with nominal dimension of 4 mm x 4 mm x 8 mm. The orientation of the crystal axis was determined in the austenitic state with a DRON-3 X-ray diffractometer using FeKα radiation. The loading axis of the

compression specimens was along the [236] crystallographic direction. Mechanical grinding followed by an electrochemical polishing (20% $HClO_4$+ 80% CH_3COOH electrolyte at T = 293 K, U = 18 V) was employed to remove any processing-affected surface layer on specimens. The mechanical tests conducted in the temperature interval 200 K < T < 550 K were performed at testing systems Instron 5969 at a strain rate $\dot{\varepsilon} = 2 \cdot 10^{-3} c^{-1}$. The microstructures were examined with a JEOL 2010 transmission electron microscopes (TEM) operated at a nominal accelerating voltage of 200 kV. Prior to the TEM observation, the 3-mm diameter disk specimens of 0.1μm in thickness were prepared and then electropolished using the twinjet method that utilized electrolyte of composition 20% H_2SO_4+80% Methanol at 10°C and 15–17 V.

3. Results and discussion

Single crystals of $Ni_{51.0}Ti_{36.5}Hf_{12.5}$ alloy are investigated in two structural states: 1) as-grown, i. e. without additional heat treatment; 2) after annealing at T=1323 K for 4 h followed by cooling at a rate of 15-25 $K \cdot min^{-1}$. In as-grown crystals a volume fraction (up to 30 %) of H-phase particles with face-centered orthorhombic lattice (Figure 1 a) is precipitated during the slow cooling in the process of single crystal growth [6, 7]. The TEM bright field image shows the H-phase particles and the characteristic satellites from four crystallographic particles variants of H-phase, including two variants of $¼[210]_{B2}$ and two variants of $⅓[110]_{B2}$ that are observed on the selected-area diffraction pattern (SAD) (Figure 1 a).

The annealing at T=1323 K results in dissolution of H-phase particles. Figure 1 b shows the TEM bright field image of B2-austenite and residual B19′-martensite after mechanical tests at T ≥ 350 K. This is confirmed by SAD pattern (inset to Figure 1 b), which does not show evidence of any additional spots or streaking that could be due to H-phase particles. Nevertheless, this problem requires additional researches by TEM and X-ray techniques, because we cannot completely exclude the precipitation of nanoscale particles of 3-5 nm during cooling after annealing at 1323 K.

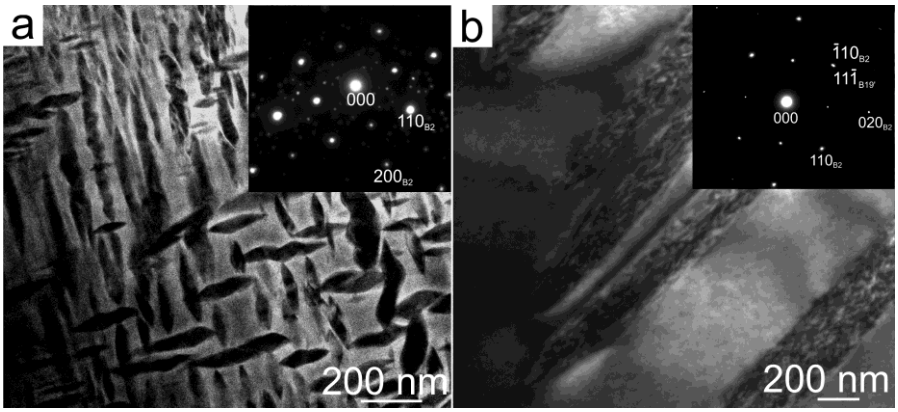

Figure 1. Transmission electron microscopy (TEM) bright field image and corresponding SAD pattern of as-grown $Ni_{51.0}Ti_{36.5}Hf_{12.5}$ single crystal, zone axis is $[001]_{B2}$ (a) and annealed at 1323K for 4 h $Ni_{51.0}Ti_{36.5}Hf_{12.5}$ single crystal, zone axis is $[001]_{B2} \| [011]_{B19'}$ (b).

Figure 2 shows the strain-temperature responses ε(T) recorded in compression tests during cooling/heating of as-grown $Ni_{51.0}Ti_{36.5}Hf_{12.5}$ single crystals oriented along [236] direction. The strain monitored during cooling/heating cycles remains at near zero for the tests with an external compressive stress magnitude |σ| from 0.3 up to 50 MPa. So, during the cooling process a self-accommodated microstructure of B19′-martensite is formed within this stress range. Under larger compressive stresses oriented martensite is grown and its volume fraction increases with external stress level. As a result reversible transformation strain ε_{rev} during cooling/heating is observed, which increases in magnitude from ε_{rev} = 0.5(±0.1) % at |σ |= 75 MPa to ε_{rev} = 0.8(±0.1) % at |σ| = 170 MPa. As expected, the martensitic start temperature (M_s) increases with the applied stress. However, for

realization of maximal recoverable strain in TiNiHf crystals the compression stress higher of 170 MPa must be applied [1, 3, 4].

In annealed $Ni_{51.0}Ti_{36.5}Hf_{12.5}$ single crystals during cooling/heating in the temperature range from 77 to 373 K under constant compressive stress from 0.3 to 170 MPa a reversible strain associated with the thermoelastic martensitic transformation is not observed. It can be due to the low martensitic start temperature M_s and high critical stress level for martensite formation in annealed single crystals.

Figures 3 and 4 show the superelastic response of [236]-oriented single crystals in as-grown and annealed states in compression. The temperature dependence of the critical stress level ($|\sigma_{cr}|(T)$) on the test temperature higher M_s for investigated single crystals is presented in Figure 5.

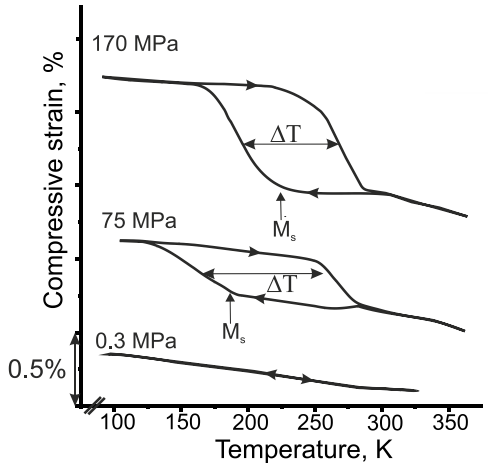

Figure 2. Strain-temperature responses of as-grown $Ni_{51.0}Ti_{36.5}Hf_{12.5}$ single crystals oriented along [236] direction during cooling/heating under constant compressive stress; ΔT is thermal hysteresis.

A linear growth in $|\sigma_{cr}|$ with increase in test temperature is observed both in as-grown and annealed states and can be described by the Clausius-Clapeyron relationship [5]:

$$\frac{d\sigma_{cr}}{dT} = -\frac{\Delta S^{A-M}}{\varepsilon_{tr}^{A-M}} = -\frac{\Delta H^{A-M}}{T_0 \varepsilon_{tr}^{A-M}}, \quad (1)$$

where $\Delta S^{A\text{-}M} < 0$ is the change of entropy associated with the forward transformation, $\Delta H^{A\text{-}M} < 0$ is the corresponding change of enthalpy, ε_{tr} is the transformation strain and T_0 is the equilibrium temperature for austenite and martensite.

It is experimentally shown that annealing at 1323 K for 4 h results in reduction of the martensitic start temperature M_s, in increase of the critical stress levels of martensite formation $|\sigma_{cr}|$ as compared to heterophase as-grown crystals (Figures 3-5). So, at T = 250 K the critical stress level of martensite formation for annealed crystals is $|\sigma_{cr}|$ = 918 MPa and it is 2.6-fold higher than $|\sigma_{cr}|$ = 350 MPa for as-grown crystals. In contrast, at higher test temperatures, the critical stress levels for the martensite formation in investigated crystals become close to each other (Figure 5). Such behavior is caused by a difference in the magnitude $\alpha = d|\sigma_{cr}|/dT$.

The annealed crystals are characterized by value twofold lower $\alpha = d|\sigma_{cr}|/dT = 4.7$ MPa·K^{-1} and wider temperature range of stress-induced martensitic transformation as compared to heterophase as-grown crystals with $\alpha = 8.6$ MPa·K^{-1} (Figure 5). As a result, the superelasticity temperature range increases almost twofold as compared to the initial crystals containing H-phase particles. Figure 5 shows superelasticity temperature ranges of ΔT^1_{SE}=75 K and ΔT^2_{SE}=135 K for crystals in as-grown and annealed states, respectively (Figures 3-5).

The analysis of σ(ε)-response shows that stress-induced martensitic transformation and superelasticity are observed at the high levels of applied compression stress from 700 to1900 MPa in $Ni_{51.0}Ti_{36.5}Hf_{12.5}$ single crystals (Figures 3 and 4). Thus, in the studied single crystals the similar inherent features of thermoelastic stress-induced martensitic transformation as in high-strength aged

NiTiHf single crystals and also binary TiNi alloys with Ni content greater than 51.3 at.% in as-grown and aged states are observed [3, 5, 8].

First, in the investigated $Ni_{51.0}Ti_{36.5}Hf_{12.5}$ single crystals the stress-induced martensitic transformation is accompanied by growth of applied compression stress with increase of given strain and σ(ε)-curves are characterized by a high strain-hardening coefficient of $\theta=\delta\sigma/\delta\varepsilon=(10\div15)x10^3$ MPa (Figures 3 and 4). A high strain-hardening coefficient θ on σ(ε)-curves for stress-induced martensitic transformation is also observed in $Ni_{50.3}Ti_{29.7}Hf_{20}$ single crystals solutionized at 1173 K for 3 h in vacuum and then quenched into water [3].

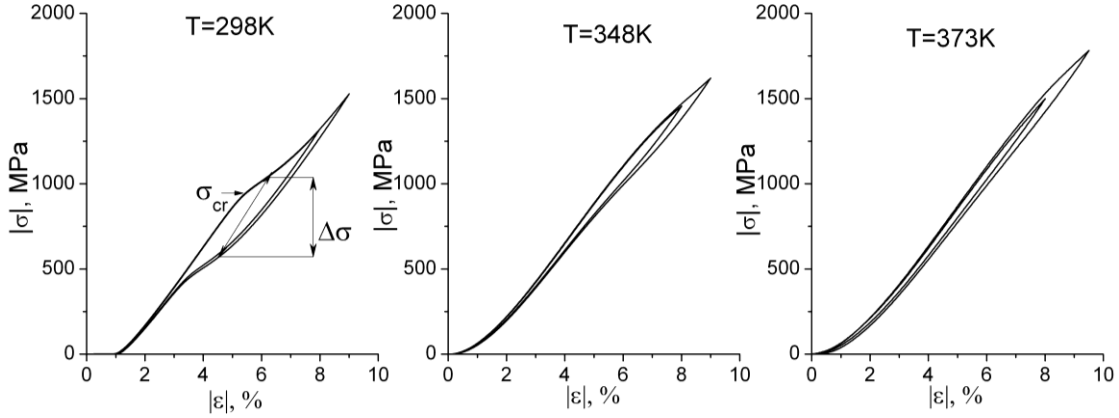

Figure 3. Stress-strain responses in compression of as-grown $Ni_{51.0}Ti_{36.5}Hf_{12.5}$ single crystals oriented along [236] direction at different test temperatures in superelasticity temperature range.

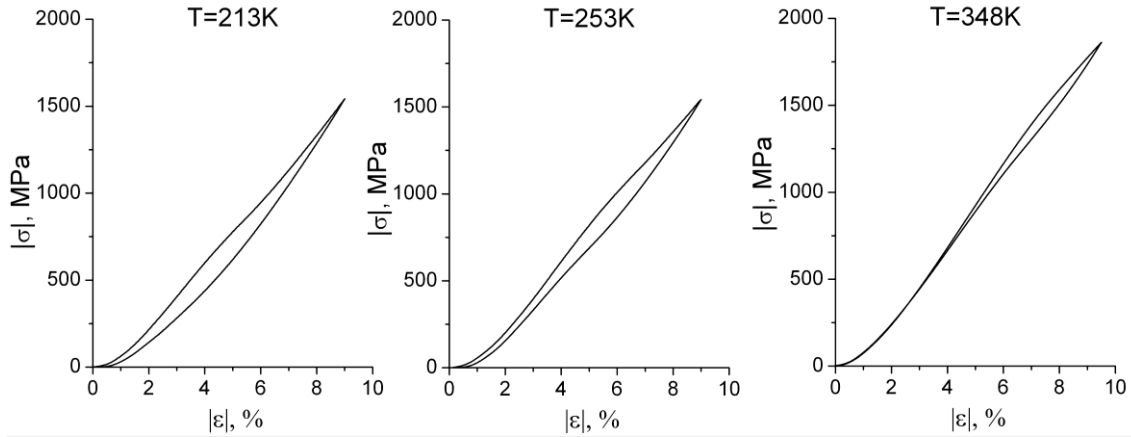

Figure 4. Stress-strain responses in compression of annealed at 1343 K for 4 h $Ni_{51.0}Ti_{36.5}Hf_{12.5}$ single crystals oriented along [236] direction at different test temperatures in superelasticity temperature range.

Second, the investigated $Ni_{51.0}Ti_{36.5}Hf_{12.5}$ crystals are characterized by a small value of reversible strain of $|\varepsilon_{SE}|=1.1\div1.4\%$ as compared to the theoretical value of lattice strain $|\varepsilon_{tr0}|_{[236]} = 8.0\%$ at B2-B19′ martensitic transformation. The strain associated with superelasticity (ε_{SE}) was defined as the maximal recoverable strain level during the stress-induced martensitic transformation. As shown in other investigations [1-4] the experimental values of reversible compression strain do not exceed of 4% in TiNiHf single crystals oriented along directions with maximal value of theoretical transformation strain of 7-8%. The third, Figures 3 and 4 illustrate a strong temperature dependence of the stress hysteresis value. The stress hysteresis Δσ was determined as the difference of stress levels between the forward and the reverse stress-induced transformation at the middle of the superelasticity

curve. Figures 3 and 4 show that value stress hysteresis in heterophase single crystals is almost twice reduced from 490 MPa down to 280 MPa with the increase of test temperature from 298 K up to 348 K. Accordingly, thermal hysteresis ΔT reduced from 100 K to 70 K with the increase of applied stress from 75 MPa to 170 MPa (Figure 2). This behaviour is typical of high-strength single crystals of binary TiNi alloys with disperse particles Ti_3Ni_4 [9].

Physical causes of small experimental values of reversible strain and reduction of stress hysteresis values with growth of the test temperature and level of applied stress require the additional researches. It is assumed that this behaviour can be caused by simultaneous action of several factors.

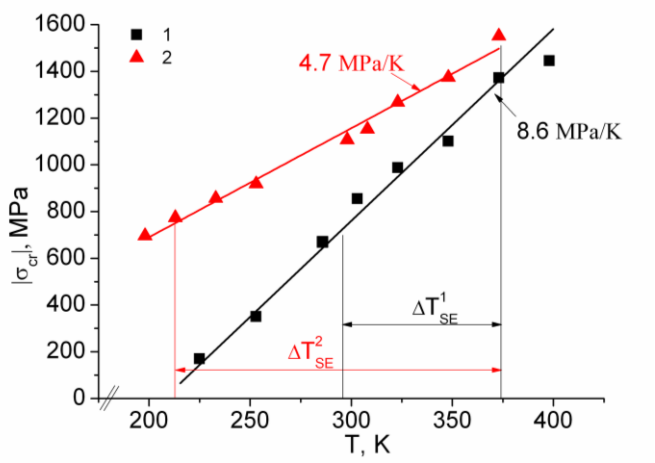

Figure 5. Temperature dependence of the critical stress level σ_{cr} of [236]-oriented $Ni_{51.0}Ti_{36.5}Hf_{12.5}$ single crystals in compression: for as-grown state (curve 1) and annealed state (curve 2).

In heterophase single crystals the decrease of transformation strain associates with the composite effect. When martensitic transformation occurs in the B2-matrix, particles of H-phase do not undergo transformation. Therefore, the volume fracture of material, which undergoes martensitic transformation and, accordingly, a value of reversible transformation strain are reduced.

Based on the thermodynamic description of stress-induced martensitic transformation external mechanical stresses ΔG_{mech}^{A-M} perform work against chemical ΔG_{ch} and non-chemical ΔG_{nonch} component of Gibbs free energy if the test temperature is higher than temperature of chemical equilibrium of phases T_0 [5, 10]:

$$\Delta G_{mech}^{A-M} = \Delta G_{ch}^{A-M} + \Delta G_{nonch}^{A-M} \quad (2)$$

Here $\Delta G_{nonch} = \Delta G_{rev} + \Delta G_{fr}$ is non-chemical contributions to the total Gibbs free energy. The non-chemical constituent is separated into reversible (elastic strain and surface) energy ΔG_{rev} and irreversible work ΔG_{fr} which is connected with overcoming friction to interfacial motion and dissipation of elastic strain energy.

In as-grown and annealed crystals the stress-induced martensitic transformation occurs with high strain-hardening coefficient θ. Therefore, for increasing the volume fraction of stress-induced martensite we have to increase the driving force of transformation to overcome the growth of the non-chemical contributions (ΔG_{rev} and ΔG_{fr}) to the total Gibbs free energy. Such a mechanism of thermoelastic martensitic transformation is usually observed at multivariant stress-induced martensitic transformation [9] and may be accompanied by the presence of non-transform volumes of austenite in the material that reduces the transformation strain.

Finally, high levels of critical stress of martensite formation from 700 up to 1900 MPa lead to occurrence of the stress-induced martensitic transformation in the conditions of strong elastic strain of austenite and martensite. The elastic compressive strain of B2-austenite along [236] direction can result in monoclinic distortion of cubic lattice and hereby in reducing the distinctions between cubic lattice of B2-phase and monoclinic B19′-martensite. Therefore, a change of austenite and martensite lattice parameters due to their elastic distortion at high critical stress level may reduce the

transformation strain and stress hysteresis value with growth of test temperature and level of critical stress at stress-induced martensitic transformations.

4. Summary

It was experimentally established that in the Ni-rich $Ni_{51.0}Ti_{36.5}Hf_{12.5}$ single crystals in as-grown and annealed at T=1323 K for 4 h states the stress-free martensitic transformation at cooling is observed at martensitic start temperature M_s below 225 K as compared to high-temperature TiNiHf alloys with low Ni content of 50.2-50.3 at.% and Hf content of 10-20 at.% [1-4]. Completely reversible stress-induced B2-B19′ martensitic transformation in [236]-oriented $Ni_{51.0}Ti_{36.5}Hf_{12.5}$ single crystals occurs at test temperature up to $T_t \sim 373$ K and high applied compressive stress up to 1700 MPa in as-grown state and 1900 MPa in annealed single crystals with value of reversible strain up to $|\varepsilon_{SE}| = 1.4\%$. The annealing at T=1323 K for 4 h of single crystals results in growth of superelasticity temperature range about twofold as compared to as-grown crystals contained disperse particles of H-phase.

Acknowledgments

Research was financially supported by Russian Science Foundation (grant No. 14-29-00012).

References

[1] Karaca H E, Saghaian S M, Basaran B, Bigelow G S, Noebe R D and Chumlyakov Y I 2011 Compressive response of nickel-rich NiTiHf high-temperature shape memory single crystals along the [111] orientation *Scripta Mater* **65** 577–580

[2] Coughlin D R, Phillips PJ, Bigelow G S, Garg A, Noebe R D and Mills M J 2012 Characterization of the microstructure and mechanical properties of a 50.3Ni–29.7Ti–20Hf shape memory alloy *Scripta Mater*. **67** 112–115

[3] Saghaian S M, Karaca H E, Tobe H, Souri M, Noebe R and Chumlyakov Y I 2015 Effects of aging on the shape memory behavior of Ni-rich $Ni_{50.3}Ti_{29.7}Hf_{20}$ single crystals *Acta Mater*. **87** 128–141

[4] Karaca H E, Saghaian S M, Ded G, Tobe H, Basaran B, Maier H J, Noebe R D and Chumlyakov Y I 2013 Effects of nanoprecipitation on the shape memory and material properties of an Ni-rich NiTiHf high temperature shape memory alloy *Acta Mater.* **61** 7422–7431

[5] Otsuka K and Ren X 2005 Physical metallurgy of Ti–Ni-based shape memory alloys *Progress in Mater. Sci.* **50** 511–678

[6] Santamarta R, Arroyave R, Pons J, Evirgen A, Karaman I, Karaca H E and Noebe R D 2013 TEM study of structural and microstructural characteristics of a precipitate phase in Ni-rich Ni–Ti–Hf and Ni–Ti–Zr shape memory alloys *Acta Mater*. **61** 6191–6206

[7] Yang F, Coughlin D R, Phillips P J, Yang L, Devaraj A, Kovarik L, Noebe R D and Mills M J 2013 Structure analysis of a precipitate phase in an Ni-rich high-temperature NiTiHf shape memory alloy *Acta Mater*. **61** 3335–3346

[8] Sehitoglu H, Jun J, Zhang X, Karaman I, Chumlyakov Y, Maier H J and Gall K 2001 Shape memory and pseudoelastic behavior of 51.5%Ni–Ti single crystals in solutionized and overaged state *Acta mater*. **49** 3609–3620

[9] Chumlyakov Y I, Kireeva I V, Panchenko E Y, Timofeeva E E, Kretinina I V and Kuts O A 2015 Physics of Thermoelastic Martensitic Transformation in High-Strength Single Crystals. *The part in the coll. monograph Shape Memory Alloys: Properties, Technologies, Opportunities*. *Trans Tech Publications* Eds: N Resnina and V Rubanik 107-174.

[10] Wollants P, Roos J R and Delaey L 1993 Thermally and stress-induced thermoplastic martenstic transformation in the reference frame of equilibrium thermodynamics *Progress in Mater. Sci.* **37** 227–288